Biochemical and Biophysical Research Communications 446 (2014) 149–154

Contents lists available at ScienceDirect

Biochemical and Biophysical Research Communications

journal homepage: www.elsevier.com/locate/ybbrc

Tumor associated osteoclast-like giant cells promote tumor growth and lymphangiogenesis by secreting vascular endothelial growth factor-C

Yu Hatano [a,b], Ken-ichi Nakahama [a,*], Mitsuaki Isobe [b], Ikuo Morita [a]

[a] Department of Cellular Physiological Chemistry, Tokyo Medical and Dental University, 1-5-45, Yushima, Bunkyo-ku, Tokyo 113-8510, Japan
[b] Department of Cardivascular Medicine, Tokyo Medical and Dental University, 1-5-45, Yushima, Bunkyo-ku, Tokyo 113-8510, Japan

ARTICLE INFO

Article history:
Received 13 February 2014
Available online 4 March 2014

Keywords:
RANKL
Osteoclast-like giant cell
VEGF-C

ABSTRACT

Tumors with osteoclast-like giant cells (OGCs) have been reported in a variety of organs and exert an invasive and prometastatic phenotype, but the functional role of OGCs in the tumor environment has not been fully clarified. We established tumors containing OGCs to clarify the role of OGCs in tumor phenotype. A mixture of HeLa cells expressing macrophage colony-stimulating factor (M-CSF, HeLa-M) and receptor activator of nuclear factor-κB ligand (RANKL, HeLa-R) effectively supported the differentiation of osteoclast-like cells from bone marrow macrophages *in vitro*. Moreover, a xenograft study showed OGC formation in a tumor composed of HeLa-M and HeLa-R. Surprisingly, the tumors containing OGCs were significantly larger than the tumors without OGCs, although the growth rates were not different *in vitro*. Histological analysis showed that lymphangiogenesis and macrophage infiltration in the tumor containing OGCs, but not in other tumors were accelerated. According to quantitative PCR analysis, vascular endothelial growth factor (VEGF)-C mRNA expression increased with differentiation of osteoclast-like cells. To investigate whether VEGF-C expression is responsible for tumor growth and macrophage infiltration, HeLa cells overexpressing VEGF-C (HeLa-VC) were established and transplanted into mice. Tumors composed of HeLa-VC mimicked the phenotype of the tumors containing OGCs. Furthermore, the vascular permeability of tumor microvessels also increased in tumors containing OGCs and to some extent in VEGF-C-expressing tumors. These results suggest that macrophage infiltration and vascular permeability are possible mediators in these tumors. These findings revealed that OGCs in the tumor environment promoted tumor growth and lymphangiogenesis, at least in part, by secreting VEGF-C.

1. Introduction

Cancer phenotype is determined not only by the biological nature of cancer cells (parenchyma), but also by cancer stroma cells [1]. Cancer stroma is composed of heterogeneous cells including endothelial cells, pericytes, fibroblasts and immune cells. Among immune cells, the accumulation of alternatively activated (M2) macrophages in cancer stroma has been considered to be an important factor in the acceleration of malignant behavior in cancers [2].

Tumor associated osteoclast-like giant cells (OGC), also a component of immune cells in cancer stroma, have been reported in a variety of organs, including the thyroid, lung, breast, stomach, liver, pancreas, gull bladder, uterus and skin [3–11]. Immunohistochemical studies revealed that OGCs have similar characteristics to osteoclasts, bone resorbing multinuclear cells. Moreover, OGC maturation was induced by macrophage colony stimulating factor (M-CSF) and the receptor activator of nuclear factor-κB ligand (RANKL), which are expressed by cancer cells themselves [12–14]. The prognostic value of tumor-associated OGCs remains controversial. Favorable prognosis has been reported in some cases of pancreatic and gastric carcinoma [8,15], although tumors containing OGCs showed aggressive behavior in pancreatic, gastric, breast, hepatic and uterine tumors [3,4,8,9,16]. Because of a lack of good model for OGC-containing tumors *in vivo*, the basic mechanism of interaction between OGCs and cancer cells is still unclear.

In the present study, we established an *in vivo* model of tumor-containing OGCs. We found that OGCs could increase macrophage infiltration, vascular permeability and lymphoangiogenesis via vascular endothelial growth factor (VEGF)-C expression. Our

* Corresponding author. Fax: +81 3 5803 0212.
E-mail address: nakacell@tmd.ac.jp (K.-i. Nakahama).

http://dx.doi.org/10.1016/j.bbrc.2014.02.113
0006-291X/

findings provide new insights into how OGCs affect the tumor microenvironment.

2. Materials and methods

2.1. Plasmid construction

The full-length cDNAs coding for the mouse RANKL (Accession No. AF019048), M-CSF (Accession No. NM_001113529), VEGF-C (Accession No. NM_009506) and Ds-Red (Clontech, USA) were amplified by polymerase chain reaction (PCR). The cDNAs of RANKL and VEGF-C were inserted into the pQCXIP (Clontech, USA). The cDNA of M-CSF was inserted into the pQCXIH, while that of Ds-Red was inserted into the pQCXIN (Clontech, USA).

2.2. Establishment of three cell lines

The HeLa cervical cancer cell line (Cell Bank, Riken, Japan, RCB0007) was cultured in Dulbecco's modified Eagle medium (DMEM, GIBCO, NZ) supplemented with 10% fetal bovine serum (10% FBS) at 37 °C, 95% humidity and 5% CO_2. HeLa cells expressing the genes (RANKL, M-CSF, VEGF-C, and Ds-Red) were established by retroviral transduction. Three cell lines were named HeLa-R (RANKL/Ds-Red), HeLa-VC (VEGF-C/Ds-Red) or HeLa-M (M-CSF/Ds-Red), respectively.

2.3. Cell proliferation assay

HeLa, HeLa-M, HeLa-R, HeLa-VC cells (1×10^4) or a mixture of HeLa-M (5×10^3) and HeLa-R (5×10^3) were seeded into 12-well flat-bottomed plates with DMEM containing 10% FBS. Cells in each sample were counted after 1-, 3-, 5- and 7-days of culture.

2.4. Osteoclastogenesis in vitro

HeLa, HeLa-M, HeLa-R (5×10^4) or a mixture of HeLa-M (2.5×10^4) and HeLa-R (2.5×10^4) were seeded onto 48-well plates with minimum essential medium alpha medium (αMEM, GIBCO, NZ) containing 10% FBS. Male ddY mice bone marrow preparations were obtained by flushing the femurs and tibias with αMEM containing 10% FBS using a 27-gauge needle. The obtained mononuclear cells (5×10^5 cells/well) were co-cultured with HeLa cells. Osteoclastogenesis was determined by tartrate-resistant acid phosphatase (TRAP) staining. Animal handling and experimental procedures were approved by the Animal Care and Use Committee of the Tokyo Medical and Dental University.

2.5. TRAP staining of the cultured cells

The TRAP staining solution was made from 0.05 M sodium acetate buffer (pH 5.0) containing naphthol AS-BI phosphate sodium salt and fast red ITR salt (Sigma Chemical, USA) in the presence of 10 mM sodium tartrate (Wako, Japan). Cultured cells were fixed with ethanol/acetone (4:1) for 1 min, left to dry for 10 min and incubated with TRAP staining solution for 30 min at 37 °C.

2.6. Tumor xenograft model

Male Tie2-GFP/Rag1$^{-/-}$ mice (6–8 weeks old, The Jackson Laboratory, USA) were purchased. HeLa, HeLa-M, HeLa-R, HeLa-VC or a mixture of HeLa-M and -R cells were suspended in DMEM containing 10% FBS and 5×10^5 cells/50 μl were dropped gently onto an Atelocollagen sponge, MIGHTY (KOKEN, Japan). After 1 h incubation, MIGHTY with cells were cultured with DMEM containing 10% FBS overnight. Tie2-GFP/Rag1$^{-/-}$ mice were anesthetized and MIGHTY including cells were implanted subcutaneously into the back. The size of tumor was measured every week and mice were sacrificed 3 or 5 weeks after the xenografts. At least three samples per cell line were harvested for histological analysis.

2.7. Histology

Tissues were fixed with 4% paraformaldehyde (PFA, Wako, Japan), dipped into 30% sucrose, embedded in an OCT compound (Tissue-Tek, USA), snap frozen in liquid nitrogen, and stored at −80 °C until use. Cryostat sections (8 μm) were incubated with a primary antibody specific to lymphatic vessel endothelial receptor 1 (LYVE-1, AngioBio, USA), CD11b (Biolegend, USA) or VEGF receptor (VEGFR)-3 (R&D, USA) overnight at 4 °C. Next, the specimens were incubated with secondary antibodies (Alexa 633- or Alexa 488-labeled antibody, Molecular probes, USA) for 30 min and images were acquired by a LSM 510 META (Carl Zeiss, Germany) or TCS-SP8 (Leica, Germany). SelecTech Staining System (Leica, USA) was used for hematoxylin eosin (HE) staining. For double-staining of LYVE-1 and TRAP, the specimens were incubated with anti-LYVE-1 antibody and visualized using a MAX-PO(R) kit (Nichirei, Japan). Additionally, the specimens were incubated for 30 min at 37 °C with TRAP staining solution.

2.8. Quantitative RT-PCR

Total RNA (5 μg) was subjected to reverse transcription using ReverTra Ace (Toyobo, Japan) and an oligo (dT) primer. The cDNA samples were amplified with Platinum SYBR Green qPCR Super Mix-UDG with ROX (Invitrogen, USA) using 7500 Real-Time PCR System (Applied Biosystems, USA). The data were analyzed by the comparative Ct Method. Primers were shown in Supplementary Table 1.

2.9. Immunoblotting analysis

The cells were lysed in a buffer containing 50 mM Tris–HCl (pH 7.5), 150 mM NaCl, 1% Triton X-100, 2 mM EDTA, 1 mM EGTA, supplemented with a protease inhibitor cocktail (Sigma, USA), and homogenized by sonication. The samples were denatured and then separated by SDS–polyacrylamide gel electrophoresis (10%). The proteins were electrotransferred to a polyvinylidene fluoride membrane (Nippon Genetics, Japan), VEGF-C immunoreactivity was detected using anti-VEGF-C antibody (Santa Cruz, USA). The band images were obtained by LAS-1000 (FUJIFILM, Japan). The blot was reprobed with an anti-β-actin polyclonal antibody (Sigma, USA) to normalize protein levels.

2.10. Immunostaining of the cells

We seeded 1×10^5 cells in a μ-Slide 8 well microscopy chamber (ibidi, Germany). After 8 h, the cells were treated with brefeldin A (Wako, Japan) overnight. After fix the cells with 4% paraformaldehyde, VEGF-C immunoreactivity was detected using anti-VEGF-C antibody and Alexa 488-labeled secondary antibody. All images were acquired by a LSM 510 META.

2.11. Vascular permeability analysis

For the vascular permeability assay, we used a tumor xenograft model as described above. Vascular permeability was analyzed three weeks after the xenograft. Thirty minutes after Evans blue dye (30 mg/kg, Sigma, USA) administration intravenously, the tumors were removed. Dissected tissues were incubated in 1 ml of

1 N KOH at 37 °C, and dye was extracted with a 4 ml extraction solution (0.6 N H_3PO_4/acetone; 5:13). The absorption at 610 nm was measured using a spectrophotometer (Gene Quant, GE, USA) for quantification.

2.12. Bone marrow macrophage chemotaxis assay

Chemotaxis of macrophages was examined using FluoroBlok 24-well Trans well migration chambers (8 μm pore size, BD Falcon, USA). Bone marrow mononuclear cells obtained from ddY mice were cultured for 5 days in αMEM containing 10% FBS and 10 ng/ml M-CSF (PeproTech, USA). On day 4, 100 ng/ml lipopolysaccharide (LPS) was added to cell culture medium. After 24 h stimulation with LPS, 1×10^5 cells were incubated with 0.5 μg/ml calcein AM (Dojindo, Japan) and added to the inserted well, while serum-free αMEM containing recombinant VEGF-C (100 ng/ml, Sigma, USA) or N-formyl-met-leu-phe (fMLP, Sigma, USA) was added to the bottom well. After 3 h, the number of migrated cells was counted under a fluorescence microscope. All assays were performed in triplicate.

2.13. Statistical analysis

SPSS 11.0.1J for Windows (SPSS Inc., USA) was used for statistical analyses. Values are shown as means ± S.E. Comparisons were made with the Student's *t*-test, and *p* values of less than 0.05 were considered significant.

3. Results

3.1. Establishement of tumor cell lines which support TRAP-positive osteoclast-like cells differentiation

We established HeLa cell lines expressing either M-CSF or RANKL (HeLa-M or -R). Thereafter, these cell lines were labeled with Ds-Red (Fig. S1). Growth rates of HeLa-M and -R were not different from parental HeLa cells (Fig. S2A). The mixture of HeLa-M and -R effectively supported TRAP-positive multinuclear cell (osteoclast-like cell) formation by co-culture with mouse bone marrow cells. However, HeLa, HeLa-M or HeLa-R alone did not support osteoclast-like cell formation (Fig. S2B).

3.2. Osteoclast-like giant multinuclear cell (OGC) formation in the tumors composed of a mixture of HeLa-M and HeLa-R

RANKL expression in the tumor environment stimulates OGC formation from monocyte/macrophage lineage cells [14]. To investigate whether established cell lines could induce OGC formation *in vivo*, these HeLa cells were implanted subcutaneously in Tie2-GFP/Rag1$^{-/-}$ mice. Five weeks after implantation, the tumors composed of a mixture of HeLa-M and -R were significantly larger than those of HeLa, HeLa-M or -R alone (Fig. 1A and B). As expected, histological analysis showed that the tumors composed of HeLa-M and -R had many TRAP-positive multinuclear OGCs, which were distributed at the marginal zone of the tumor (Fig. 1C).

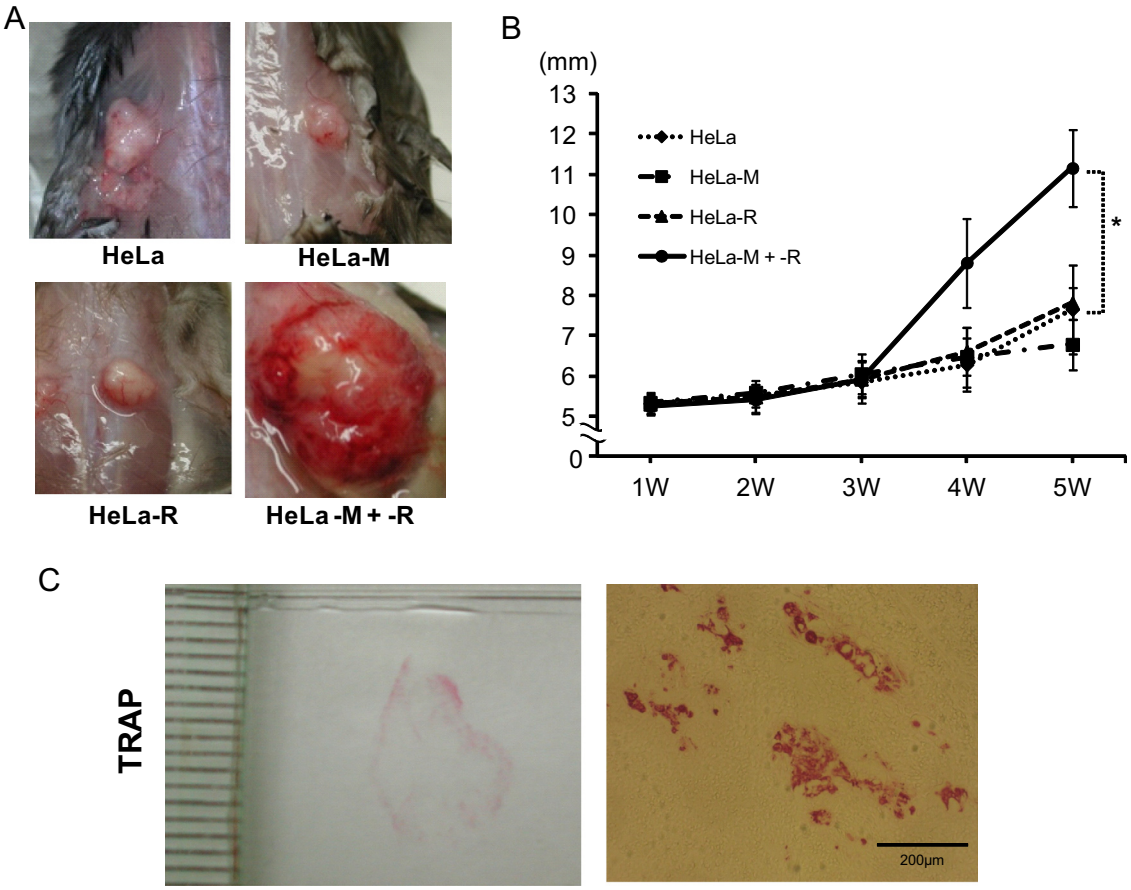

Fig. 1. A tumor composed of HeLa-M and -R stimulated OGC formation and grew larger. (A) Four images showed tumor appearance at 5 weeks after each HeLa cell line xenograft. Images were taken after removing the skin at the same magnitude. (B) Tumor growth curve drawn by measuring the long axis of the formed tumors at the indicated times. Values are presented as means ± S.E. $n = 5$, $^*p < 0.05$ vs HeLa. (C) Representative macroscopic (left) and microscopic (right) images of a TRAP-stained specimen obtained from a tumor composed of HeLa-M and -R at 5 weeks after xenograft. TRAP-positive cells were distributed at the marginal zone of the tumor.

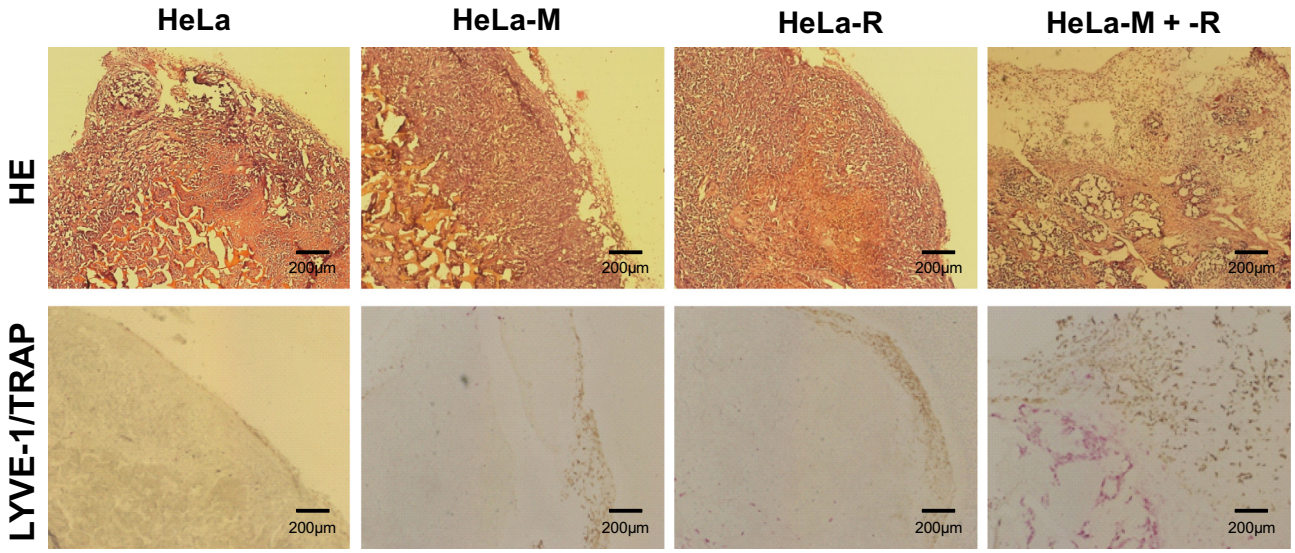

Fig. 2. A tumor containing OGCs accelerates lymphangiogenesis. Tumors composed of each cell line were obtained at 5 weeks after xenografting and stained with HE or LYVE-1/TRAP using a double-staining method. Increased peritumoral lymphangiogenesis was observed in the tumors composed of HeLa-M and -R.

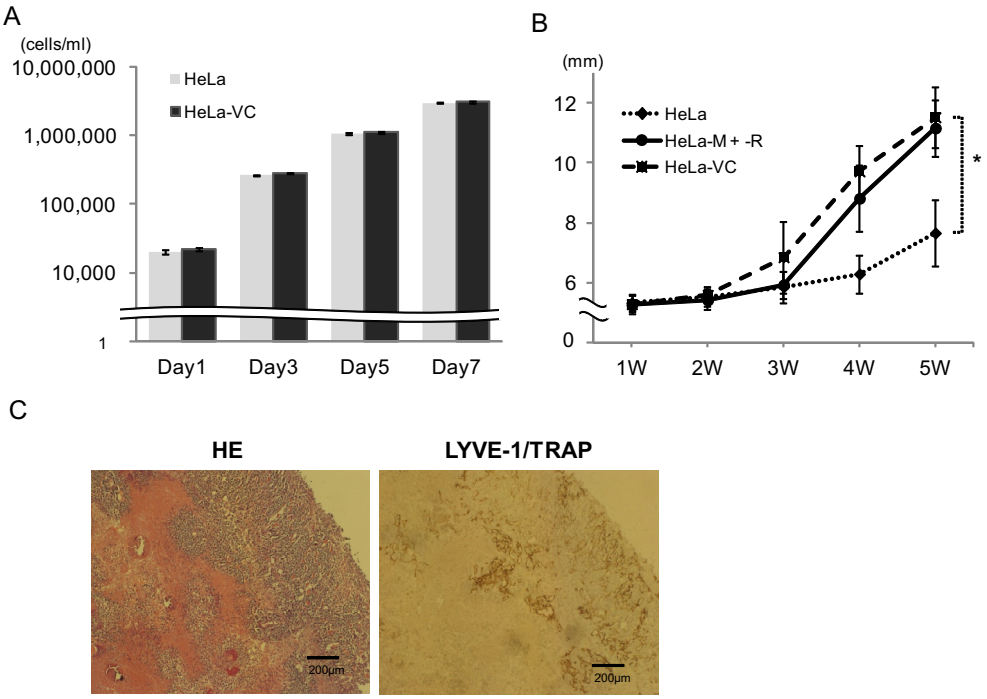

Fig. 3. A tumor composed of HeLa-VC also promoted tumor growth similar to OGC-containing tumors. (A) The graph shows *in vitro* cell proliferation of HeLa and HeLa-VC. The vertical axis shows a logarithmic scale and the difference was not significant between the two cell lines. Values are presented as means ± S.E. $n = 3$. (B) Growth curve of a tumor in xenograft model. Diameter of the formed tumors were measured at the indicated times. Values are presented as means ± S.E. $n = 5$, $^{*}p < 0.05$ vs HeLa. (C) Representative microscopic images of the tumor at 5 weeks after the xenograft stained with HE or LYVE-1/TRAP double-staining. The tumors composed of HeLa-VC contained many lymphatic vessels without OGC formation.

3.3. Enhanced lymphangiogenesis in the tumors containing OGCs

To clarify the mechanism by which OGCs induced tumor growth, histological analysis was performed. It was reported that osteoclasts secrete VEGF-C. Moreover, we confirmed a positive relationship between VEGF-C production and osteoclast-like cell formation *in vitro* (Fig. S3). VEGF-C has been shown to induce tumor lymphangiogenesis and facilitate tumor spread to the regional lymph nodes in animal tumor models. Therefore, we next examined the involvement of lymphangiogenesis in the tumors containing OGCs. Increased peritumoral lymphangiogenesis close to OGC areas was observed in the tumors composed of HeLa-M and -R as compared with that of HeLa, HeLa-M or HeLa-R (Fig. 2 and Fig. S4). The receptor for VEGF-C, VEGFR-3, expression was detected on LYVE-1 positive lymphatic vessels but not on HeLa cells (Fig. S5A).

3.4. Similar phenotype of tumors composed of VEGF-C secreting HeLa cells to those containing OGCs

To investigate the effect of VEGF-C on tumor growth, we established VEGF-C overexpressing HeLa cells. VEGF-C protein expression was confirmed by Western blotting analysis and immunohistochemistry (Fig. S6). Although cell proliferation was not affected *in vitro* (Fig. 3A), tumor growth was accelerated by VEGF-C expression and tumor growth in HeLa-VC tumors resembled that of the tumors containing OGCs *in vivo* (Fig. 3B). As expected, the tumors composed of HeLa-VC contained many lymphatic vessels without OGC formation (Fig. 3C). Distribution of lymphatic vessels was intraparenchymal and different from that of the tumors containing OGCs (Fig. 3C and Fig. S4). HE staining showed acellular lesion inside the tumor. This result may indicate lymphatic fluid accumulation (Fig. 3C).

3.5. Up-regulation of vascular permeability and chemotaxis of macrophages could be one mechanism in the accelerated tumor growth of VEGF-C

To determine mechanisms underlying the links between accelerated tumor growth and VEGF-C, we evaluated vascular permeability and macrophage chemotaxis. As expected, vascular permeability significantly increased in the tumors composed of the mixture of HeLa-M and -R ($p = 0.04$), and to some extent in HeLa-VC ($p = 0.08$), in comparison with that of HeLa (Fig. 4A). Macrophage infiltration is thought to promote tumor growth, so we next assessed CD11b$^+$ macrophage recruitment into tumors. The tumors composed of a mixture of HeLa-M and -R contained a larger amount of CD11b$^+$ macrophages than that of HeLa. Almost all CD11b$^+$ macrophages expressed VEGFR-3 (Fig. S5B) and CD11b$^+$ macrophage recruitment was also observed in the tumors of HeLa-VC (Fig. 4B). We found that recombinant VEGF-C promoted LPS-stimulated bone marrow macrophage chemotaxis *in vitro* (Fig. 4C).

4. Discussion

In the present study, we established an *in vivo* model to examine the effect of OGCs on the tumor microenvironment. To our knowledge, there has been no report demonstrating an experimental tumor model that supports osteoclast-like cell formation. OGCs in tumors have similar characteristics to osteoclasts [17]. The mixed culture of HeLa-M and HeLa-R effectively supported osteoclastogenesis, although each alone did not support osteoclastogenesis *in vitro*. This result led us to examine the effect of OGCs on the tumor microenvironment. A Xenograft model of these cells showed that the tumors consisting of HeLa-M and HeLa-R contained OGCs and developed to a larger size than those of HeLa, HeLa-M or HeLa-R. This result indicates that a certain factor secreted from OGCs may affect tumor size. An immunohistological

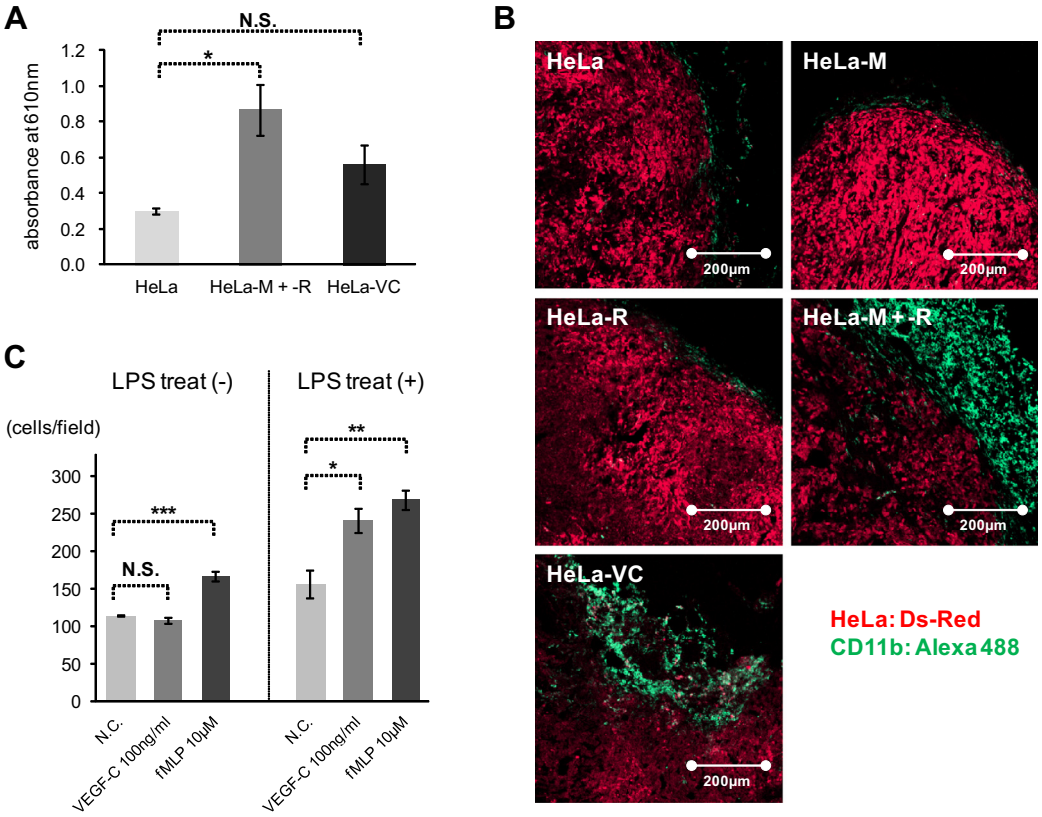

Fig. 4. A tumor of HeLa-VC and a mixture of HeLa-M and -R showed accelerated vascular permeability. OGC-containing tumors recruited CD11b+ macrophages *in vivo* and VEGF-C promoted BMM chemotaxis *in vitro*. (A) Quantitative assay of vascular permeability by the absorption at 610 nm is shown. Vascular permeability increased significantly in the tumors composed of the mixture of HeLa-M and -R ($p = 0.04$), and to some extent in HeLa-VC ($p = 0.08$), in comparison with that of HeLa. Values are presented as means ± S.E. $n = 3$, $^*p < 0.05$ vs HeLa. (B) Representative immunofluorescence images of a tumor at 5 weeks after a xenograft composed of each HeLa cell line. CD11b was detected by a specific primary antibody and Alexa 488-conjugated secondary antibody (green). HeLa cells express Ds-Red genetically (red). The tumors composed of a mixture of HeLa-M and -R contained a larger amount of CD11b$^+$ macrophages than that of HeLa, and CD11b$^+$ macrophage recruitment was also observed in the tumors of HeLa-VC. (C) BMM chemotaxis toward VEGF-C was evaluated using FluoroBlok 24-well Trans well migration chambers (8 μm pore size). Recombinant VEGF-C (100 ng/ml) promoted LPS-stimulated BMM chemotaxis. The macrophage chemoattractant fMLP (10 μM) was used as a positive control. Values are presented as means ± S.E. $n = 3$, $^*p < 0.05$, $^{**}p < 0.01$, $^{***}p < 0.001$ vs N.C. (For interpretation of the references to color in this figure legend, the reader is referred to the web version of this article.)

study clearly showed enhanced lymphangiogenesis around the tumors containing OGCs. Moreover, VEGF-C expression was upregulated with osteoclast-like cells differentiation *in vitro*. In xenograft experiments, OGCs were observed at marginal zones of tumors and VEGFR-3 positive lymphatic vessels surrounded these OGC areas, while lymphatic vessels penetrated into the tumors composed of HeLa-VC. These results strongly suggested that VEGF-C was responsible for lymphangiogenesis in the tumors containing OGCs. Increased expression of VEGF-C in the tumor environment induces lymphangiogenesis and is associated with metastasis to lymph nodes and/or other organs, leading to poor prognosis [18–21]. Therefore, OGCs could be an important factor in the acceleration of malignant cancer phenotypes.

Another finding of our study was the involvement of VEGF-C in tumor growth. VEGF-C has been reported as a lymphangiogenic and angiogenic factor by interaction with its receptor VEGFR-3 and VEGFR-2 [22]. A previous report showed that both VEGF-C and VEGFR-3 were expressed by HeLa cell lines and contributed to HeLa cell growth [23]. In this study, HeLa cells used in our experiments expressed neither VEGF-C nor VEGFR-3 and the growth rate of HeLa-VC was not different from parental HeLa cells *in vitro*. The functions of VEGF-C were reported to be promotion of vascular permeability and macrophage mobilization, in addition to lymphangiogenesis [24,25]. Our results showed that vascular permeability increased in OGC-containing tumors, but not in VEGF-C overexpressing tumors. VEGF-C expression in tumors may help promote vascular permeability, but lymphatic vessels in VEGF-C overexpressing tumors were not fully functional, so interstitial pressure could increase and partly counteract vascular permeability [26]. VEGF-C-dependent macrophage recruitment could be another mechanism underlying tumor progression. Recently, it was reported that not only lymphatic endothelial cells, but also monocyte/macrophage lineage cells expressed VEGFR-3 [27,28]. Tumor-associated macrophages secrete a number of mitogenic cytokines and growth factors which lead to proliferation of tumor cells, and moreover, tumor-associated macrophage infiltration correlates with increased growth of tumors and poor prognosis [29]. Our data and previous reports showed VEGF-C induced VEGFR-3-dependent chemotaxis of macrophages [24]. Therefore, VEGF-C could be a chemoattractant for macrophages and contribute to tumor growth aggressively.

In conclusion, our study established an *in vivo* OGC maturation model, and OGCs in the tumor environment accelerated the growth of tumors independent of M-CSF or RANKL. A lymphangiogenic factor, VEGF-C, was upregulated with differentiation of osteoclast-like cells from a monocyte/macrophage lineage and OGCs promoted lymphatic vessel formation in a xenograft model. Our results suggest that vascular permeability and macrophage chemotaxis could be possible mechanisms for the accelerated tumor growth due to VEGF-C. RANKL-OGC axis is a new approach to controlling the cancer environment and will contribute to clinical treatment.

Appendix A. Supplementary data

Supplementary data associated with this article can be found, in the online version, at http://dx.doi.org/10.1016/j.bbrc.2014.02.113.

References

[1] Y. Mao, E.T. Keller, D.H. Garfield, K. Shen, J. Wang, Stromal cells in tumor microenvironment and breast cancer, Cancer Metastasis Rev. 32 (2013) 303–315.
[2] N.B. Hao, M.H. Lu, Y.H. Fan, Y.L. Cao, Z.R. Zhang, S.M. Yang, Macrophages in tumor microenvironments and the progression of tumors, Clin. Dev. Immunol. 2012 (2012) 948098.
[3] A. Aru, P. Norup, B. Bjerregaard, B. Andreasson, T. Horn, Osteoclast-like giant cells in leiomyomatous tumors of the uterus. A case report and review of the literature, Acta Obstet. Gynecol. Scand. 80 (2001) 371–374.
[4] V. Stracca-Pansa, A. Menegon, P.M. Donisi, L. Bozzola, F. Fedeli, F. Quarto, O. Nappi, G. Pettinato, Gastric carcinoma with osteoclast-like giant cells. Report of four cases, Am. J. Clin. Pathol. 103 (1995) 453–459.
[5] N. Al-Brahim, S. Salama, Malignant melanoma with osteoclast-like giant cells: an unusual host response: immunohistochemical and ultrastructural study of three cases and literature review, Am. J. Dermatopathol. 27 (2005) 126–129.
[6] T.J. Bocklage, D. Dail, T.V. Colby, Primary lung tumors infiltrated by osteoclast-like giant cells, Ann. Diagn. Pathol. 2 (1998) 229–240.
[7] B.S. Serezhin, N.M. Anichkov, L. Avdeenko Iu, Anaplastic thyroid carcinoma with osteoclast-like giant cells, Arkh. Patol. 59 (1997) 50–53.
[8] K.H. Molberg, C. Heffess, R. Delgado, J. Albores-Saavedra, Undifferentiated carcinoma with osteoclast-like giant cells of the pancreas and periampullary region, Cancer 82 (1998) 1279–1287.
[9] M. Ahaouche, D. Cazals-Hatem, D. Sommacale, J.F. Cadranel, J. Belghiti, C. Degott, A malignant hepatic tumour with osteoclast-like giant cells, Histopathology 46 (2005) 590–592.
[10] T. Akatsu, K. Kameyama, S. Kawachi, M. Tanabe, K. Aiura, G. Wakabayashi, M. Ueda, M. Shimazu, M. Kitajima, Gallbladder carcinoma with osteoclast-like giant cells, J. Gastroenterol. 41 (2006) 83–87.
[11] P. Viacava, A.G. Naccarato, V. Nardini, G. Bevilacqua, Breast carcinoma with osteoclast-like giant cells: immunohistochemical and ultrastructural study of a case and review of the literature, Tumori 81 (1995) 135–141.
[12] B.M. Kacinski, CSF-1 and its receptor in ovarian, endometrial and breast cancer, Ann. Med. 27 (1995) 79–85.
[13] H.O. Smith, P.S. Anderson, D.Y. Kuo, G.L. Goldberg, C.L. DeVictoria, C.A. Boocock, J.G. Jones, C.D. Runowicz, E.R. Stanley, J.W. Pollard, The role of colony-stimulating factor 1 and its receptor in the etiopathogenesis of endometrial adenocarcinoma, Clin. Cancer Res. 1 (1995) 313–325.
[14] C.L. Gibbons, S.G. Sun, M. Vlychou, K. Kliskey, Y.S. Lau, A. Sabokbar, N.A. Athanasou, Osteoclast-like cells in soft tissue leiomyosarcomas, Virchows Arch. 456 (2010) 317–323.
[15] K. Suda, M. Takase, T. Oyama, T. Mitsui, S. Horike, An osteoclast-like giant cell tumor pattern in a mucinous cystadenocarcinoma of the pancreas with lymph node metastasis in a patient surviving over 10 years, Virchows Arch. 438 (2001) 519–520.
[16] R. Holland, U.J. van Haelst, Mammary carcinoma with osteoclast-like giant cells. Additional observations on six cases, Cancer 53 (1984) 1963–1973.
[17] G.J. Atkins, D.R. Haynes, S.E. Graves, A. Evdokiou, S. Hay, S. Bouralexis, D.M. Findlay, Expression of osteoclast differentiation signals by stromal elements of giant cell tumors, J. Bone Miner. Res. 15 (2000) 640–649.
[18] J. Krishnan, V. Kirkin, A. Steffen, M. Hegen, D. Weih, S. Tomarev, J. Wilting, J.P. Sleeman, Differential in vivo and in vitro expression of vascular endothelial growth factor (VEGF)-C and VEGF-D in tumors and its relationship to lymphatic metastasis in immunocompetent rats, Cancer Res. 63 (2003) 713–722.
[19] S.J. Mandriota, L. Jussila, M. Jeltsch, A. Compagni, D. Baetens, R. Prevo, S. Banerji, J. Huarte, R. Montesano, D.G. Jackson, L. Orci, K. Alitalo, G. Christofori, M.S. Pepper, Vascular endothelial growth factor-C-mediated lymphangiogenesis promotes tumour metastasis, EMBO J. 20 (2001) 672–682.
[20] M.M. Mattila, J.K. Ruohola, T. Karpanen, D.G. Jackson, K. Alitalo, P.L. Harkonen, VEGF-C induced lymphangiogenesis is associated with lymph node metastasis in orthotopic MCF-7 tumors, Int. J. Cancer 98 (2002) 946–951.
[21] M. Skobe, T. Hawighorst, D.G. Jackson, R. Prevo, L. Janes, P. Velasco, L. Riccardi, K. Alitalo, K. Claffey, M. Detmar, Induction of tumor lymphangiogenesis by VEGF-C promotes breast cancer metastasis, Nat. Med. 7 (2001) 192–198.
[22] K. Plate, From angiogenesis to lymphangiogenesis, Nat. Med. 7 (2001) 151–152.
[23] X. Shi, G. Chen, H. Xing, D. Weng, X. Bai, D. Ma, VEGF-C, VEGFR-3, and COX-2 enhances growth and metastasis of human cervical carcinoma cell lines in vitro, Oncol. Rep. 18 (2007) 241–247.
[24] M. Skobe, L.M. Hamberg, T. Hawighorst, M. Schirner, G.L. Wolf, K. Alitalo, M. Detmar, Concurrent induction of lymphangiogenesis, angiogenesis, and macrophage recruitment by vascular endothelial growth factor-C in melanoma, Am. J. Pathol. 159 (2001) 893–903.
[25] A. Saaristo, T. Veikkola, B. Enholm, M. Hytonen, J. Arola, K. Pajusola, P. Turunen, M. Jeltsch, M.J. Karkkainen, D. Kerjaschki, H. Bueler, S. Yla-Herttuala, K. Alitalo, Adenoviral VEGF-C overexpression induces blood vessel enlargement, tortuosity, and leakiness but no sprouting angiogenesis in the skin or mucous membranes, FASEB J. 16 (2002) 1041–1049.
[26] A.K. Alitalo, S.T. Proulx, S. Karaman, D. Aebischer, S. Martino, M. Jost, N. Schneider, M. Bry, M. Detmar, VEGF-C and VEGF-D blockade inhibits inflammatory skin carcinogenesis, Cancer Res. (2013).
[27] P. Hamrah, L. Chen, C. Cursiefen, Q. Zhang, N.C. Joyce, M.R. Dana, Expression of vascular endothelial growth factor receptor-3 (VEGFR-3) on monocytic bone marrow-derived cells in the conjunctiva, Exp. Eye Res. 79 (2004) 553–561.
[28] K.L. Hall, L.D. Volk-Draper, M.J. Flister, S. Ran, New model of macrophage acquisition of the lymphatic endothelial phenotype, PLoS ONE 7 (2012) e31794.
[29] C.E. Lewis, J.W. Pollard, Distinct role of macrophages in different tumor microenvironments, Cancer Res. 66 (2006) 605–612.